



# Application of expanding probe electrical resistivity method in delineating leachate contamination zone at Farri Open Dumpsite, IJEBU ODE, Southwestern Nigeria

Ganiyu Omotola Mosuro<sup>a</sup>, Jean Eniola Usman<sup>a</sup>, Olateju Olatunji Bayewu<sup>a</sup>,  
Oluwadamilare Oluwatobiloba Odugbesan<sup>b</sup>, Moroof Olasunbo Oloruntola<sup>c</sup>  
and Kuburat Olukemi Bakare<sup>d</sup>

<sup>a</sup>Department of Earth Sciences, Olabisi Onabanjo University, Ago Iwoye, Nigeria; <sup>b</sup>Department of Earth and Environmental Sciences, Tulane University, New Orleans, LA, USA; <sup>c</sup>University of Lagos, Lagos, Nigeria; <sup>d</sup>Department of Geological Services, Ministry of Industry, Trade and Investment, Oke-Mosan, Abeokuta, Nigeria

## ABSTRACT

An evaluation of subsurface contamination in the Farri dumpsite area of Ogun State, Southwestern Nigeria, has been carried out with the aim of determining the degree of contamination and infiltration of leachate into the subsurface soil using the vertical electrical sounding (VES) method. Twenty VES points were probed using the Schlumberger array with a current electrode spacing (AB/2) of 80 m. The resistivity values recorded were processed via the partial curve matching approach, and modelling with WINRESIST software was employed to generate the geoelectric parameters of the subsurface. The interpretation of the data obtained shows the presence of three underlying lithological layers with Q and H geophysical curve type geometry. The lithological layer present in the study area includes topsoil, clayey, sandy clayey and compacted sandy layer with resistivity values ranging from 10.9 to 1091.3  $\Omega\text{m}$ , 11.4 to 110.9  $\Omega\text{m}$ , 141.7 to 275.6  $\Omega\text{m}$  and 1293.7 to 9880.9  $\Omega\text{m}$ . Overburden thickness varies from 0.5 to 3.2 m across the study area. Three contamination categories (uncontaminated, moderately contaminated and contaminated) were adopted for rating contamination. The geospatial representation of the calculated longitudinal conductance shows that the protective capacity is low in the northwestern part, moderate within the central region, and high in the southeastern and southern parts of the study area.

## ARTICLE HISTORY

Received 18 August 2021  
Revised 2 January 2023  
Accepted 9 December 2024

## KEYWORDS

Leachate; Contamination;  
Electrical; protective  
capacity; Porosity

## 1. Introduction

The urbanisation rate in Nigeria in recent decades has been linked to population growth and the need for industrialisation, which has resulted in the disposal of waste into the environment (Ibitola et al. 2011). Inhabitants of most areas in countries such as Nigeria, where there are no proper environmental laws guiding waste disposal, dispose of their waste in available area. This is due to their limited knowledge about the effects of improper waste disposal on the environment (Aboh 2001; Abdullahi et al. 2013). This continuous demand for more space for the disposal of these domestic and industrial wastes from urban areas makes waste disposal a necessary part of the human cycle of activities (Meju 2000). Statistically, in 2020, Nigeria recorded an estimate of over 32 million tons of solid waste yearly (Bakare 2020).

The interaction between the inhomogeneous dumpsite materials, the soils and the subsurface geologic units affects the underground water resources, consequently constituting a high risk to

humans and the environment. It is also expected that the organic matter decomposing at dumpsites would have generated enough leachate plume over the years, which could have infiltrated and polluted the groundwater in the area (Bayode et al. 2011; Smith 1992).

Mapping the contamination of leachate over an area requires the adoption of appropriate exploration techniques, either passively or actively. Appropriate geophysical methods and logging have been found useful for the determination of boundaries of a landfill site and fill thickness. The nature of abandoned solid waste landfills can also be investigated and, hence, eliminate potential hazards (Oluwafemi 2012).

The consideration of the development of the study area, Farri dumpsite, southwestern Nigeria, necessitates this research aimed at investigating the leachate-contaminated regions of the subsurface lithology, by delineating the subsurface lithological layers and outlining regions that are leachate filled and leachate free in order to assess possible present and future effects in the study area. The variation in

the depth of leachate contamination in the area will serve as a model to delineate the subsurface lithology and map the leachate-free and leachate-filled regions of the subsurface.

## 2. Location and geology of the study area

Farri dumpsite is located in Ijebu-Ode, Southwestern Nigeria, between longitudes  $3^{\circ}56'16''$ – $3^{\circ}56'32''$ E and latitudes  $6^{\circ}47'23''$ – $6^{\circ}47'34''$ N. The area is accessible via the Shagamu-Benin expressway and a well-connected footpath and minor road (Figure 1). The historical satellite image of Farri Dumpsite, presented in Figure 2(A–D), shows a gradual expansion in the land area due to an increase in refuse disposal from 2015 to 2021. The satellite image of the dumpsite in 2015 shows limited disposal of refuse, while 2017 shows a little presence of dump. The satellite image of 2019 and 2021 shows a greater concentration of dump in the entire region of the Farri Dumpsite in 2021. The increase in the dump land use indicates a growing use of the dumpsite over time, with approximate physical dump region area coverage of 22,262, 24,157, 31,624 and 46,090 sq-m for 2015, 2017, 2019 and 2021, respectively. Geographically, the area is characterised by the

tropical rain forest belt of southwestern Nigeria, with a monsoon climate of high temperatures, high rainfall, high evapotranspiration and high relative humidity forming important factors in the water balance, with a mean annual rainfall of about 1750 mm. The temperature varies with the season, ranging from about  $23^{\circ}\text{C}$  to  $25^{\circ}\text{C}$  during the wet season and  $23^{\circ}\text{C}$  to  $30^{\circ}\text{C}$  in the dry season. The mean relative humidity varies from 66.2% in January to 88.4% in July (Akanni et al. 2000; Onakomaiya et al. 1992).

Geologically, the study location falls within the Dahomey sedimentary basin of the Abeokuta Formation, which is stratigraphically divided into three recognisable formations: Ise Formation, Afowo Formation and Araromi Formation, overlying one another, with geological ages of Albian, Turonian and Maastrichtian, respectively (Billman 1976; Omatsola and Adegoke 1981). These formations form an unconformity on the crystalline Precambrian Basement rock (Okosun 1990; Obaje 2009; Okeke et al. 2019).

## 3. Methodology

This research adopts an integrated approach cutting across the soil sampling in holes and the geophysical

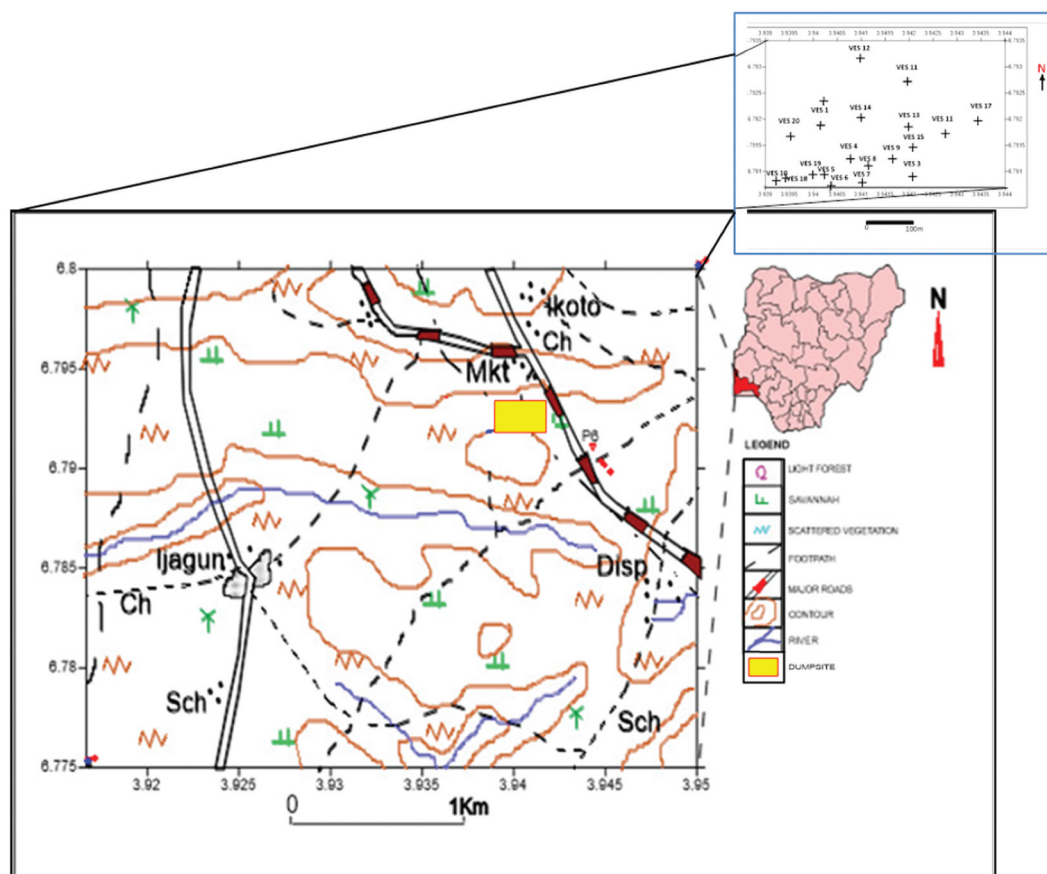


**Figure 1.** Basemap of the study area, illustrating both human and natural features. The inset map in the upper-right corner highlights the location of the surveyed points.

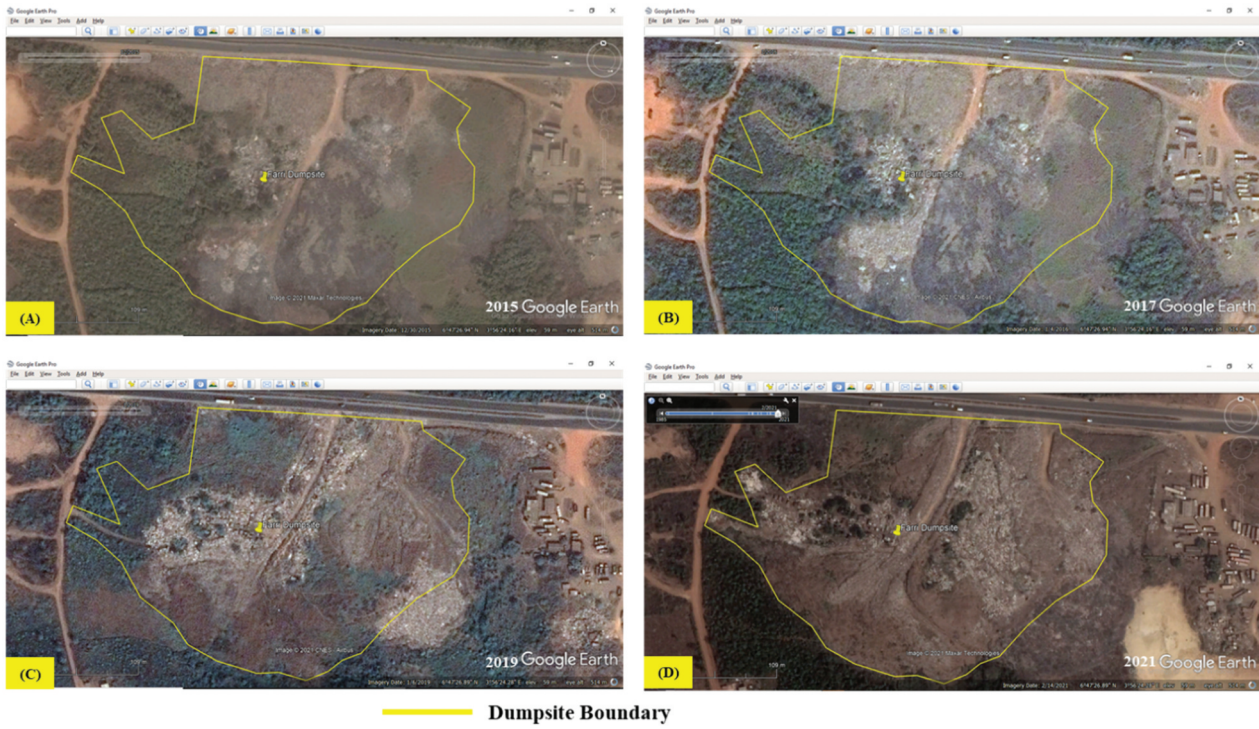


**Figure 2.** Historical satellite images of the study area (adapted from Google Earth) for the years 2015, 2017, 2019 and 2021 to show the evolution of the dumpsite with respect to land use.

field of geoscience. The soil in the study area was sampled using an Auger for two points, which were spatially distributed to regions of physical presence or absence of leachate observation. The equipment components were coupled as needed and secured with screws to obtain 6 m depth length to mechanically excavate and transport soil recovery. The soft nature of the sandy soil underlying the study area provides a rapid hole drilling through the soil. The properties of the soil recovery were carefully observed and noted on the field.

An electrical resistivity survey using the Schlumberger array was adopted to establish a total of 20 vertical electrical sounding (VES) points across the dumpsite, with a maximum current electrode spacing ( $AB/2 = 80$  m) with the aid of a highly sophisticated, compact Ohmega Resistivity Meter with an inbuilt power source, aluminium electrodes, two cables reels of 200 m length used in connecting current electrodes ( $C_1$  and  $C_2$ ) while two reels with cables of 50 m in length used in connecting potential electrodes ( $P_1$  and  $P_2$ ). The obtained resistance result was multiplied by the geometric factor (GF) as define in Equation (i), to determine the apparent resistivity value (Blaricom 2002; Reynolds 2003). This value was further processed using the RESIST version 1.0 software through a process known as computer iteration.

$$\text{Apparent Resistivity } (\rho_a) = \left( \frac{\left(\frac{AB}{2}\right)^2 - \left(\frac{MN}{2}\right)^2}{MN} \right) \times \pi \quad (i)$$

( $\rho_a$  = resistivity ( $\Omega m$ ),  $AB$  = current electrode spacing (m),  $MN$  = potential electrode spacing (m),  $\pi = 3.142$ ).

The resistivity values and thickness of the subsurface layer were used in the computation of the longitudinal conductance, which is a geophysical parameter that determines the vertical behaviour of the subsurface to the current passing through it. The mathematical approach for longitudinal conductance value computation is presented in Equation (ii), after Henriot (1976).

$$\text{Total Longitudinal Conductance (S)} = \sum \left( \frac{h_1}{\rho_1} \right) + \left( \frac{h_2}{\rho_2} \right) + \dots + \left( \frac{h_n}{\rho_n} \right) \quad (ii)$$

where,

$\Sigma$  is a summation sign,  $h_i$  is the thickness of the  $i$ th layer and  $\rho_i$  is the resistivity of the  $i$ th layer.

This geo-electric parameter provides information on the ability of the underlining subsurface lithology to hold contaminant from affecting the aquiferous unit or any other lithological unit of interest. The longitudinal conductance has been linked to overburden protective capacity classification by Henriot (1976) (Table 1).

The established geoelectric depth from VES from the current electrode spread to that of the subsurface depth was correlated by applying the mathematical approach depth conversion factor provided in Equation (iii) by (Gholam and Mohammad 2005)



**Table 1.** Longitudinal conductance/protective capacity rating (after Henriët 1976).

Total longitudinal unit conductance ( $\Omega^{-1}$ )	Overburden protective capacity classification
<0.10	Poor
0.1–0.19	Weak
0.2–0.69	Moderate
0.7–1.0	Good

$$Depth = 0.57 \left( \frac{AB}{2} \right)^{0.97} \quad (\text{iii})$$

The results of the calculated apparent resistivity values obtained and the derived longitudinal conductance values were used to produce the geospatial representation of the calculated geoelectric parameters in the study area, using Surfer 16 Golden Software and a minimum curvature gridding method.

The inference of the lithology of the subsurface within the study area was achieved with the correlation of the range of resistivity values obtained with the core recovery lithology with respect to the local geologic setting of the study area, since the properties of the underlying lithology determine the behaviour (conductance or resistance) of electric current

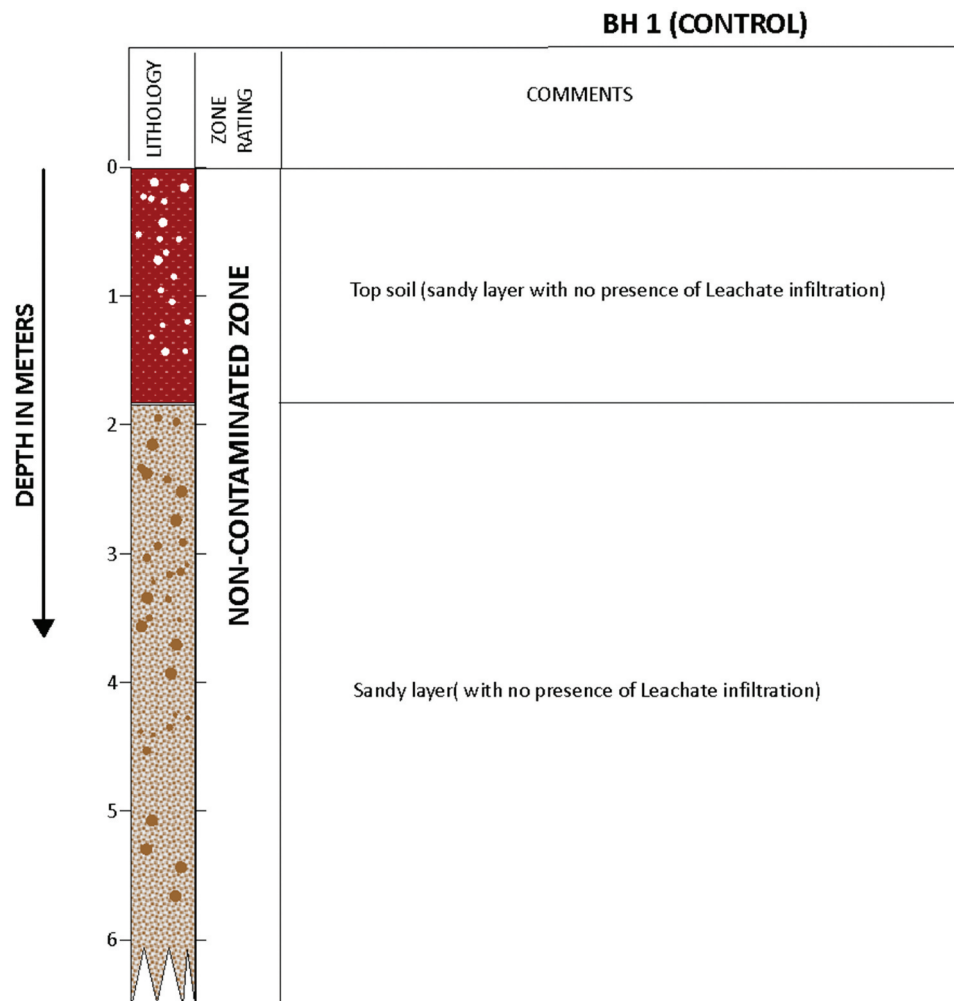
travelling through them. The established borehole core serves an essential guide for the calibration of depth, lithology and soil models.

## 4. Results and discussion

### 4.1. Lithological description

The lithologs and descriptions are based on two cored holes in the affected area. The cored holes are drilled to a depth of between 5 and 6 m, respectively. The lithofacies in the two cored holes are topsoil, clayey layer, fine-to-medium-grained sands and compacted sands, with refuse waste as the topsoil in the area. Borehole 1 of the study area is established in the control region of the study area, which is situated 200 m from the dumpsite. The core recovery process reveals that the underlying lithology in the control location is composed of clean sandy layer with no leachate presence (Figure 3), while the core borehole log within the dumpsite premises reveals contaminated sand with the presence of leachate (Figure 4).

The consideration of the lithological recovery from the logging for the depth of 0–6 m and the obtained geoelectric parameters (Table 2) from the depth of 0–

**Figure 3.** Lithological log of Borehole 1 describing the lithological characteristics.



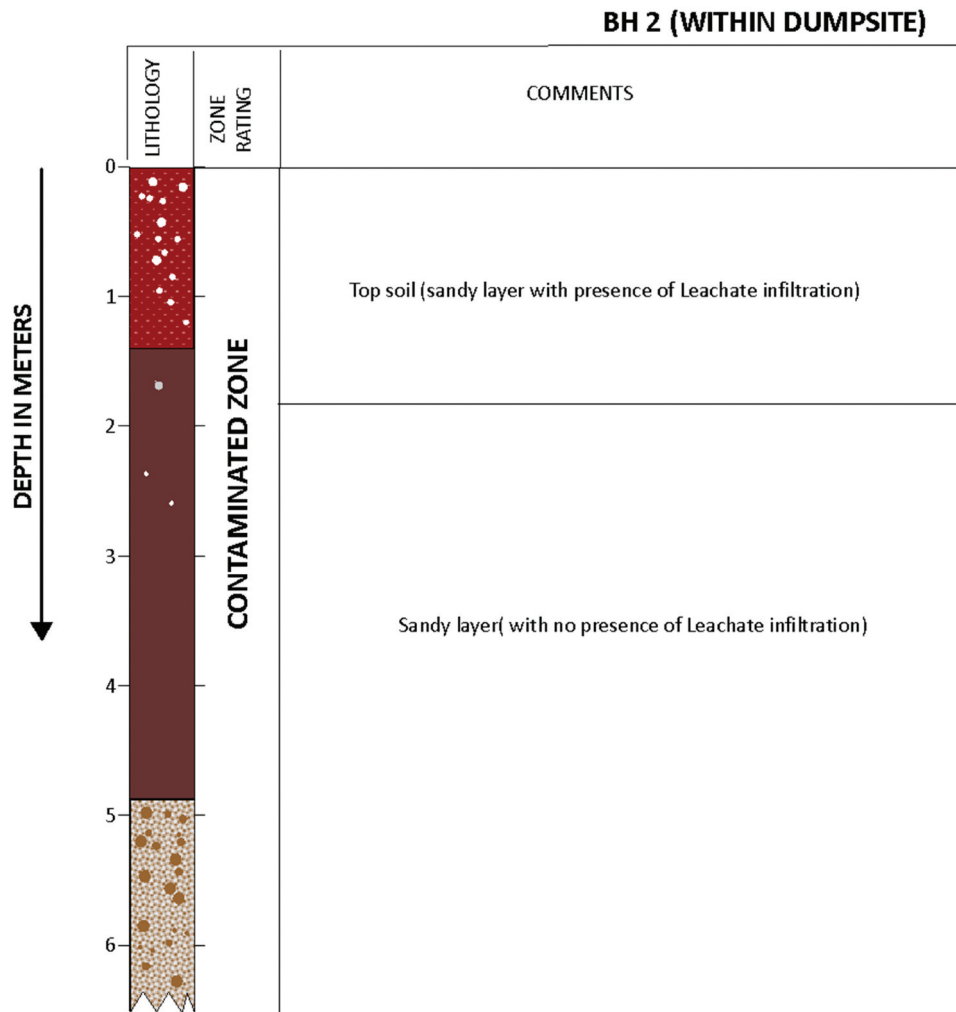


**Figure 4.** Lithological log of Borehole 2 describing the lithological characteristics.

80 m reveals that the geophysical curves (Figure 5a-c) shows the area is underlain by (3) three lithological layers with varying lithological nature spatially. VES 1 and 9 display an A curve type, VES 7 and 8 display a K curve type while VES 2, 3, 4, 5, 6, 8 and 10–20 display an H curve type. The lithological layer present in the study area includes topsoil, clayey, sandy clayey and compacted sandy layer, with resistivity values ranging from 10.9 to 1,091.3  $\Omega\text{m}$ , 11.4 to 110.9  $\Omega\text{m}$ , 141.7 to 275.6  $\Omega\text{m}$  and 1,293.7 to 9,880.9  $\Omega\text{m}$ , respectively.

The geoelectric section of the subsurface lithological layer for VES 3, 15, 13 and 11 in Figure 6 reveals correlated lithological layer between the established points, but there is variation in the depth of the lithological layer occurrence. The topsoil layer resistivity ranges from 40.2 to 262.7  $\Omega\text{m}$ , with a depth of 1.1–3.2 m. The clayey layer shows resistivity values ranging from 11.4 to 117.4  $\Omega\text{m}$ . VES 3 and 13 have thicknesses of 3.3 and 9.1 m, respectively. The compacted sand layer shows high resistivity values, ranging from 1293.7 to 9880.9  $\Omega\text{m}$ .

#### 4.2. Contaminated region investigation

In mapping the spatial contamination variation in the area, the degrees of contamination at specific depths are considered based on the respective resistivity values. The electrical resistivity varies between different geological materials depending mainly on variations in water content and dissolved ions in the water (Samouëlian et al. 2005). Resistivity investigations can thus be used to identify zones with different electrical properties, which can then be referred to different geological strata. The presence of clay minerals strongly affects the resistivity of sediments and weathered rock (Yusuf and Abiye 2019). Clay minerals may be regarded as electrically conductive particles that can absorb and release ions and water molecules on their surface through an ion exchange process. The current electrode spacing of  $AB/2 = 1.0, 4.0$  and  $9.0$  m corresponding to  $0.6, 2.4$  and  $5.4$  m real depths, respectively, were used to determine the contamination rate within the subsurface lithology (Table 3).

**Table 2.** Geoelectric parameters and inferred lithology of the VES points established within the study area.

VES No.	Resistivity ( $\Omega\text{m}$ )	Thickness (m)	Depth (m)	Inferred Lithology	Curve Type
1	370.5	1.9	1.9	Top soil	A
	2100.1	8.9	10.8	Sandy	
	4089.4			Compacted Sand	
2	1091.3	1.5	1.5	Top soil	H
	694.5	4.1	5.5	Sandy	
	3357.9			Compacted Sand	
3	262.7	1.5	1.5	Top soil	H
	117.4	3.3	4.9	Clayey	
	9880.9			Compacted Sand	
4	42.3	1.1	1.1	Top soil	H
	29.7	4	5.1	Clayey	
	308.7			Sandy	
5	31.2	1.2	1.2	Top soil	H
	12.9	3.2	4.4	Clayey	
	738.2			Sandy	
6	63.7	0.5	0.5	Top soil	H
	23.4	5.6	6.1	Clayey	
	1482.6			Sandy	
7	293.6	1	1	Top soil	K
	1884.8	3	4	Compacted Sand	
	414.3			Sandy	
8	204.7	1.9	1.9	Top soil	H
	130.3	18.3	20.2	Sandy Clay	
	782.7			Sandy	
9	472.6	1	1	Top soil	A
	1622.1	7.9	8.9	Sandy	
	2655.3			Compacted Sand	
10	604.6	1.5	1.5	Top soil	H
	243.6	7.4	8.9	Sandy	
	4533.1			Compacted Sand	
11	50.5	1	1	Top soil	H
	15.2	4.6	5.6	Clayey	
	2013.6			Compacted Sand	
12	141.6	1	1	Top soil	H
	185.1	3.1	4.1	Sandy Clay	
	1430.2			Sandstone	
13	186.4	3.2	3.2	Top soil	H
	99.1	9.1	12.3	Clayey	
	2863.4			Compacted Sand	
14	18.2	1.1	1.1	Top soil	H
	41.3	4.5	5.6	Clayey	
	294.3			Sandy	
15	40.2	1.2	1.2	Top soil	H
	11.4	3.6	4.8	Clayey	
	1293.7			Compacted Sand	
16	28.8	0.9	0.9	Top soil	H
	18.8	4.6	5.5	Clayey	
	258.3			Sandy Clay	
17	44.6	1	1	Top soil	H
	22.3	8.3	9.3	Clayey	
	141.7			Sandy Clay	
18	10.9	1	1	Top soil	H
	110.9	2.7	3.8	Clayey	
	143.9			Sandy Clay	
19	142.5	1.1	1	Top soil	H
	275.6	7.3	8.4	Sandy Clay	
	626.7			Sandy	
20	153.8	1	1	Top soil	H
	57.9	4.1	5.1	Clayey	
	405.4			Sandy	

#### 4.2.1. Contamination determination at 0.6 m

The degree of contamination was determined at a current electrode spread (AB/2) of 1.0 m, with respect to the electrical behaviour of the subsurface lithological unit. The resistivity values range between 6.04 and 625.06  $\Omega\text{m}$ . The 2D and 3D iso-resistivity map at 1.0 m depth (Figure 7) shows that

the resistivity is very low towards the southwestern and northeastern parts of the study area, and the resistivity within this layer generally increases towards the northeastern and southeastern parts of the study area. Areas with low resistivity values are generally believed to be leachate filled/contaminated. The established VES points 1, 4, 5,

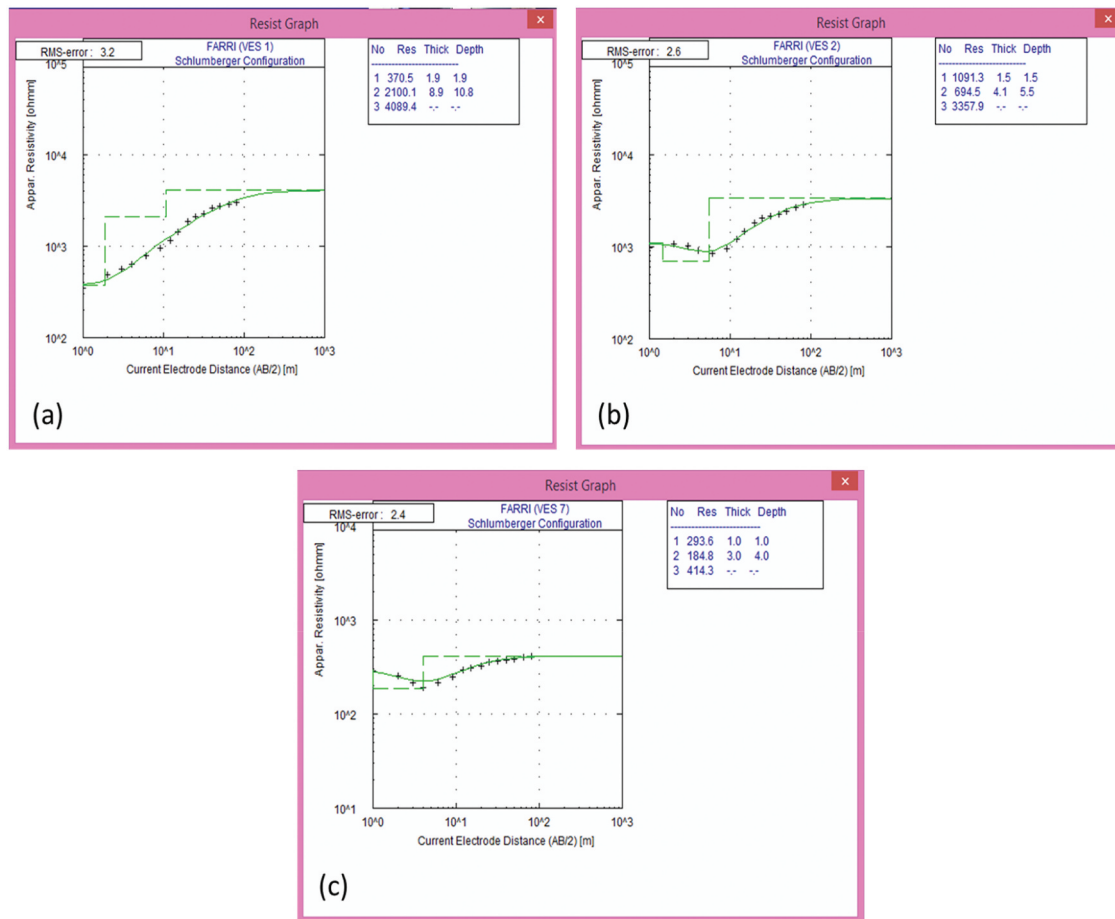


**Figure 5.** Iterated geoelectric curves and generated parameters for VES points 1, 2, and 7, representing A, H, and K-type curves, respectively. The green lines highlight the model's best fit, characterized by the lowest root mean square (RMS) error.

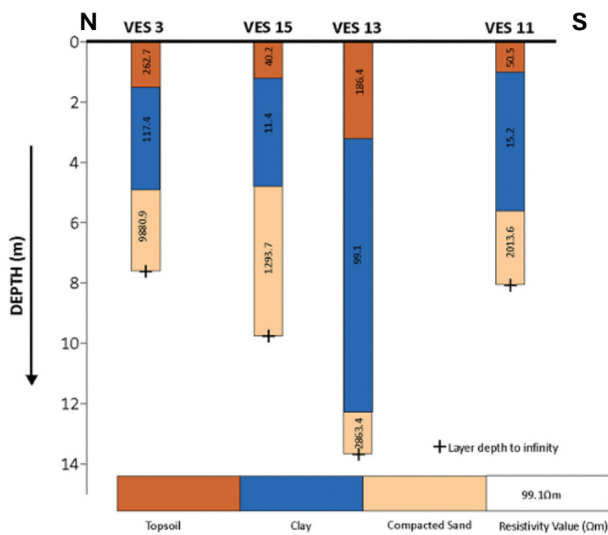


**Figure 6.** Geoelectric section of VES traverse along south-north direction.

6, 7, 8, 10, 11, 12, 13, 14, 15, 16, 17, 18, 19 and 20 are leachate-filled areas, while VES 2, 3 and 9 are leachate-free regions (Table 2).

#### 4.2.2. Contamination determination at 2.6 m

The contamination rate was inferred from the recorded resistivity values at a current electrode spread (AB/2) of 4.0 m, with resistivity values at this depth level ranging from 10.56 to 1113.68  $\Omega\text{m}$ . VES 1, 3, 7 and 8 are moderately contaminated with leachate, and VES 4, 5, 6, 11, 12, 15, 16, 17, 19 and 20 are contaminated (Table 2). The generated geospatial resistivity variation using 2D and 3D resistivity maps at 4.0 m depth in Figure 8 reveals that resistivity is very low towards the southwestern part of the study area, and the resistivity within this layer generally increases towards the central, northeastern and south-eastern parts of the study area. Areas with low resistivity values are generally believed to be leachate filled and contaminated.

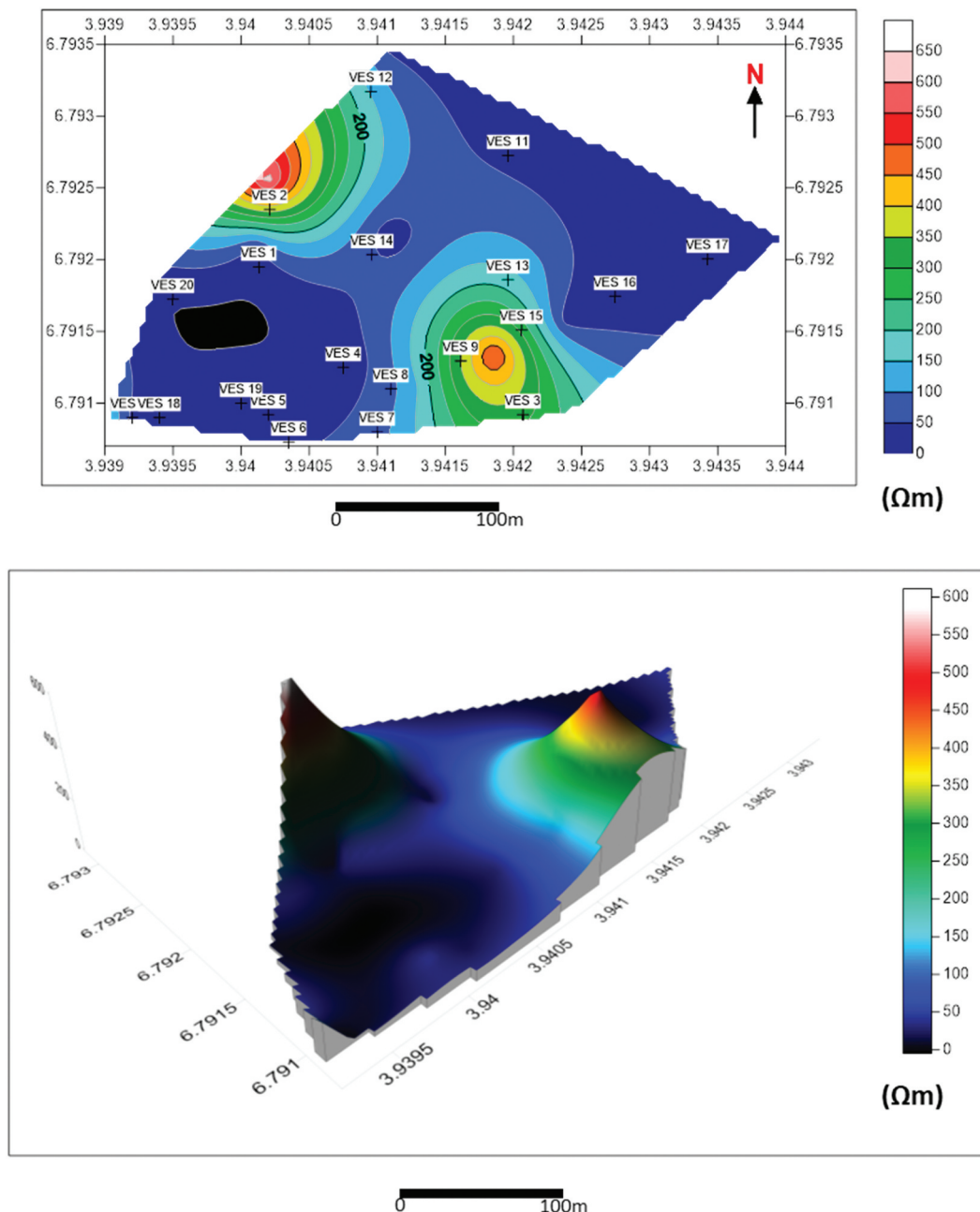
#### 4.2.3. Contamination determination at 5.4 m

The resistivity values recorded at a current electrode (AB/2) spacing of 9.0 range from 11.0 to 18,074.76  $\Omega\text{m}$  at this depth level, indicating a low to high range of resistivity values. The generated 2D and 3D iso-resistivity map shows that the resistivity is generally



**Table 3.** Contamination rate characterisation of the subsurface at depths 1.0, 4.0 and 9.0 m.

VES No.	at AB/2 = 1.0 m		at AB/2 = 4.0 m		at AB/2 = 9.0 m	
	Resistivity ( $\Omega$ m)	Contamination Description	Resistivity ( $\Omega$ m)	Contamination Description	Resistivity ( $\Omega$ m)	Contamination Description
1	45.87	Contaminated	238.06	Moderately Contaminated	857.05	Uncontaminated
2	625.06	Uncontaminated	1113.68	Uncontaminated	955.5	Uncontaminated
3	237.42	Uncontaminated	127.69	Moderately Contaminated	418.89	Uncontaminated
4	28.74	Contaminated	30.66	Contaminated	54.37	Contaminated
5	21.18	Contaminated	19.62	Contaminated	32.35	Contaminated
6	45.63	Contaminated	13.28	Contaminated	31.31	Contaminated
7	108.58	Moderately Contaminated	272.91	Moderately Contaminated	51	Contaminated
8	126.49	Moderately Contaminated	224.84	Moderately Contaminated	177.37	Moderately Contaminated
9	508.89	Uncontaminated	795.2	Uncontaminated	1413.71	Uncontaminated
10	175.56	Moderately Contaminated	476.72	Uncontaminated	328.82	Contaminated
11	17.16	Contaminated	10.56	Contaminated	11	Contaminated
12	38	Contaminated	47.53	Contaminated	331.35	Uncontaminated
13	88.25	Contaminated	445.17	Uncontaminated	120.13	Moderately Contaminated
14	21.66	Contaminated	685.54	Uncontaminated	1934.59	Uncontaminated
15	28.99	Contaminated	37.52	Contaminated	25.42	Contaminated
16	11.63	Contaminated	16.73	Contaminated	45.72	Contaminated
17	52.08	Contaminated	69.26	Contaminated	105.37	Moderately Contaminated
18	7.93	Contaminated	185.98	Uncontaminated	559.95	Uncontaminated
19	42.33	Contaminated	22.53	Contaminated	25.8	Contaminated
20	6.04	Contaminated	65.62	Contaminated	18074.76	Uncontaminated

**Figure 7.** 2D and 3D iso-resistivity map at a depth of 0.6 m (AB/2 = 1.0 m).

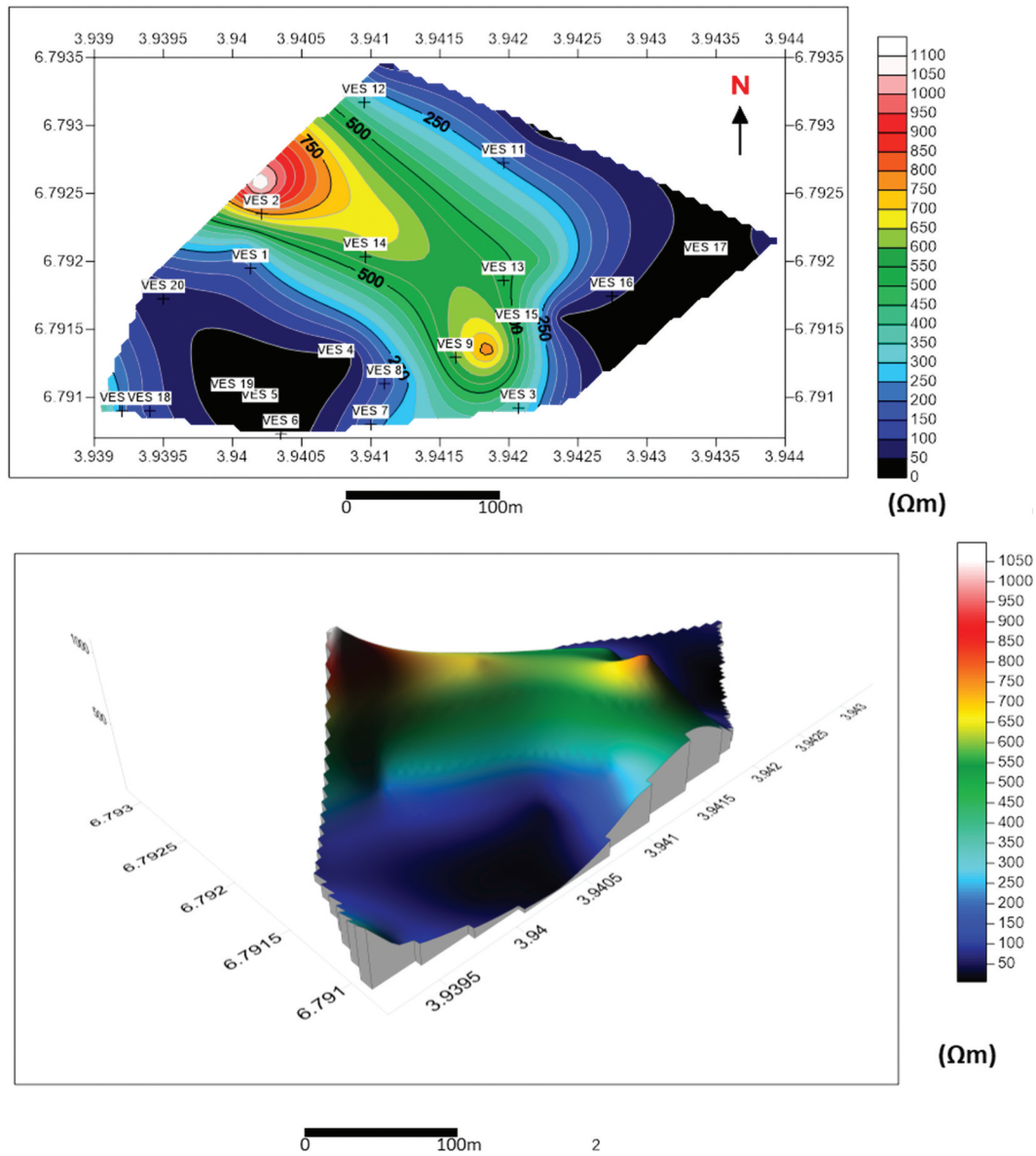


**Figure 8.** 2D and 3D iso-resistivity map at a depth of 2.4 m ( $AB/2 = 4.0$  m).

moderate to high at this depth level, except in some portions of the northwestern and southwestern parts of the study area (Figure 9). Hence, areas with low resistivity values are generally believed to be leachate filled/contaminated. The established level shows that VES 4, 5, 6, 7, 8, 11, 12, 13, 15, 16, 17 and 19 are leachate-filled areas, while VES 1, 2, 3, 9, 10, 14, 18 and 20 are leachate-free regions. VES 8, 13 and 17 are moderately contaminated with leachate, and VES 4, 5, 6, 7, 10, 11, 15, 16 and 19 are contaminated (Table 2). Visualising the degree of contamination within the study area at different depths, a stacked map was used to show the variation in the resistivity

values in Figure 10. This map clearly shows that the degree of contamination within the study area decreases with depth from 0.6 to 5.4 m.

#### 4.3. Protective capacity

The computed longitudinal conductance and protective capacity classification of the established VES points in Farri Dumpsite are presented in Table 4. The longitudinal conductance value ranges from 0.001 to 0.45 mhos, which is a typical value falling into three major protective capacity classifications. Grouping the calculated

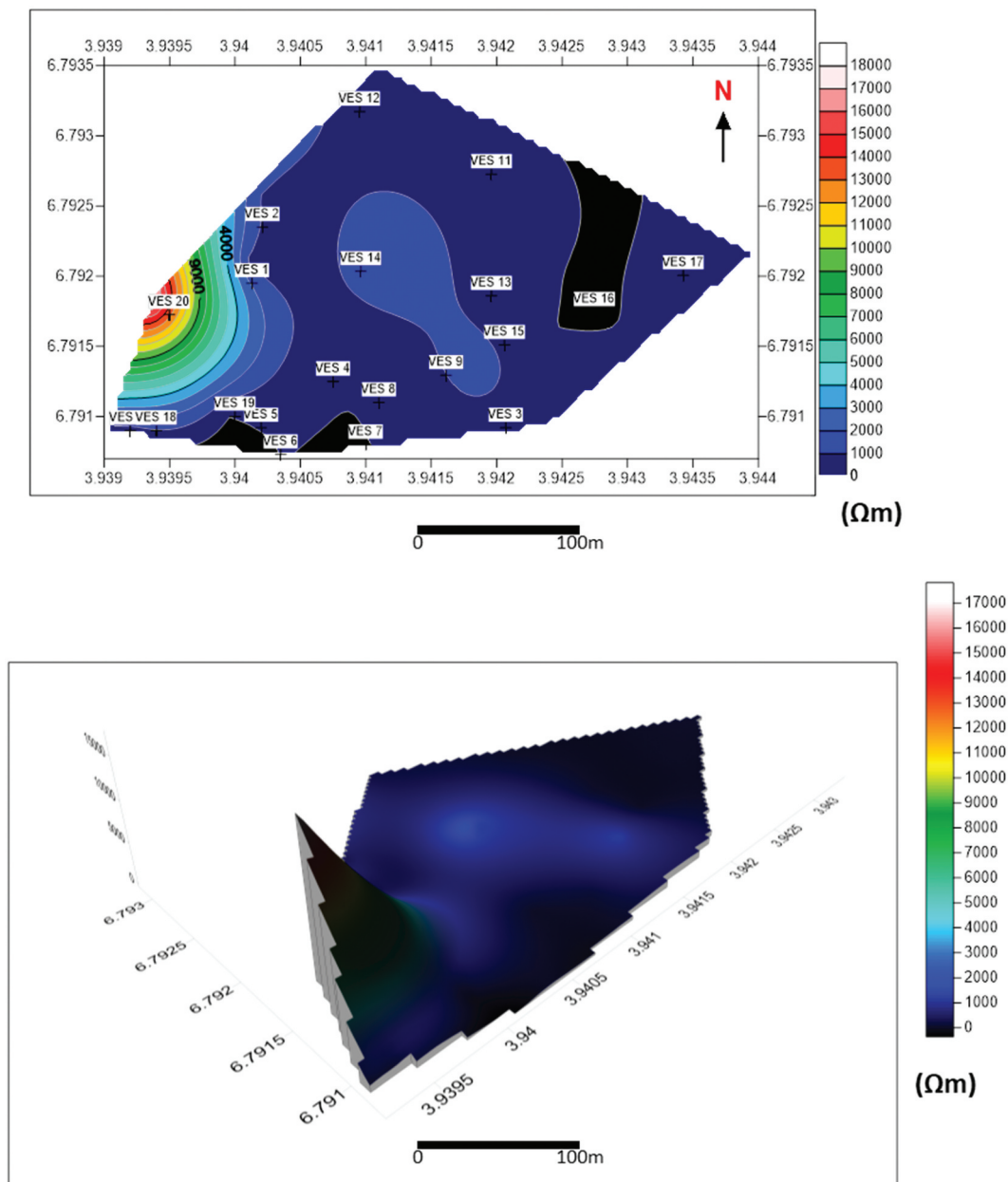


**Figure 9.** 2D and 3D iso-resistivity map at a depth of 5.4 m ( $AB/2 = 9.0$  m).

longitudinal conductance values for the delineation of the protective capacity reveals that the poor, weak and moderate classifications occur at nine, three and eight locations, indicating percentages of 45%, 15% and 40%, respectively (Figure 11). The protective capacity at a depth of 0.6 m is weak, allowing the movement of leachate across the lithological sandy unit due to its high porosity and also the shallowness of this depth to the surface. The protective capacity at a depth of 4.0 is also considered poor to moderate because of the presence of sandy layer, but at a less shallow depth compared to 1.0 m. The protective capacity at a depth of 9.0 m reveals moderate protective capacity. The geospatial representation of the protective capacity of the established point is

presented in a 2D geospatial map (Figure 12), which shows the spatial variation in the overburden layer's protective capacity to withstand contamination from the surface. The northwestern and southeastern regions have poor and weak protective capacity, while the central region has moderate protective capacity. The previous hydrogeological investigation in the study area has established the average depth to the water level to be  $>25.0$  m (Ayolab and Badmus 2004). The consideration of the recorded contamination depth infiltration level in this previous research (Mosuro et al. 2019; Adebisi et al. 2022) and the recorded level of leachate infiltration in this research reveals a considerable level of safety for the aquiferous layer from infiltration.



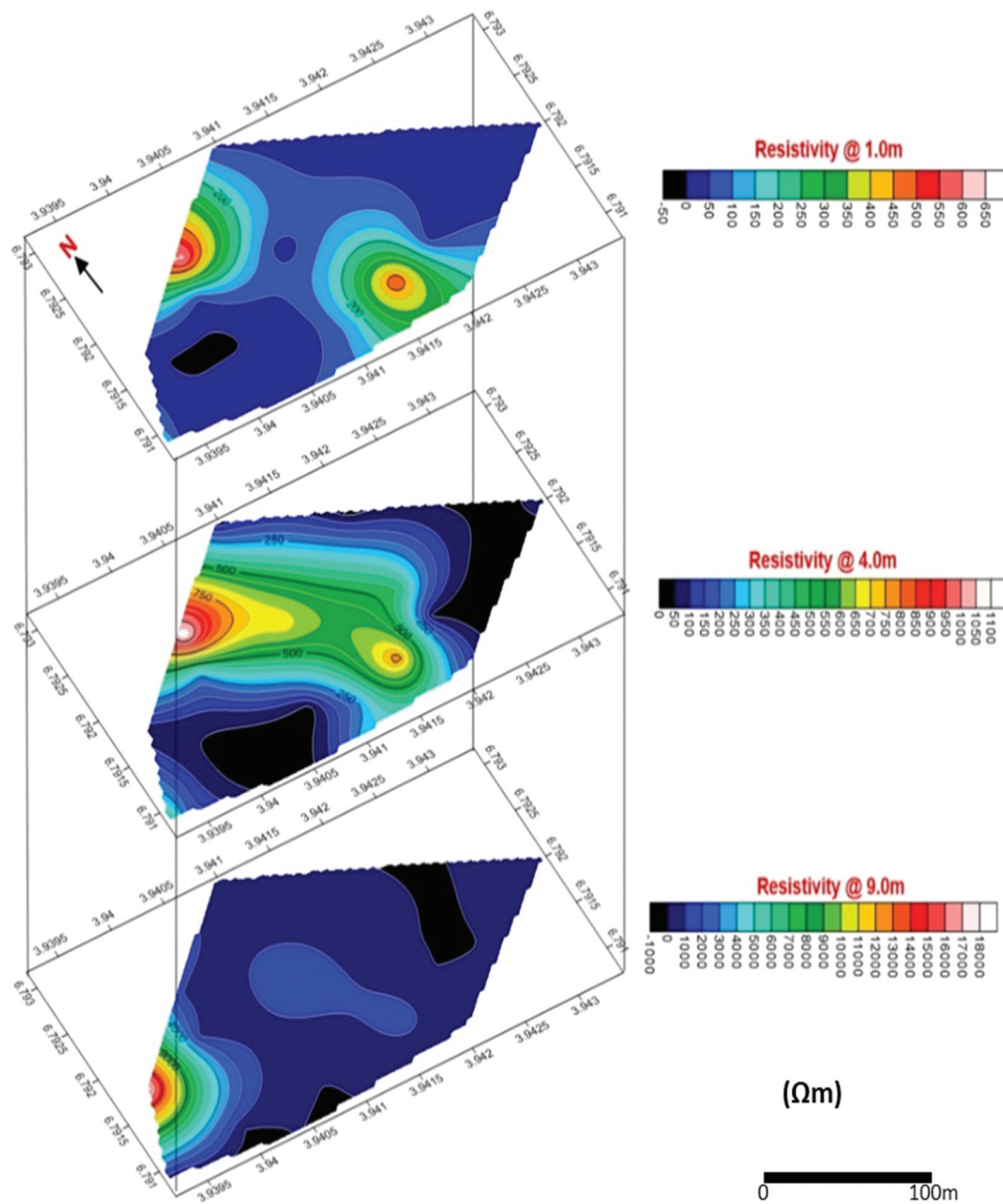


**Figure 10.** Stacked map of iso-resistivity at depths of 1.0 m, 4.0 m, and 9.0 m (Figures 7–9), showing the vertical variation in electrical resistivity across the study area.

**Table 4.** Computed longitudinal conductance and protective capacity classification of the established VES point in the study location.

VES No.	Longitudinal Conductance ( $\Omega^{-1}$ )	Protective Capacity Rating
VES 1	0.01	Poor
VES 2	0.01	Poor
VES 3	0.05	Poor
VES 4	0.20	Moderate
VES 5	0.38	Moderate
VES 6	0.27	Moderate
VES 7	0.01	Poor
VES 8	0.16	Weak
VES 9	0.01	Poor
VES 10	0.04	Poor
VES 11	0.39	Moderate
VES 12	0.03	Poor
VES 13	0.14	Weak
VES 14	0.20	Moderate
VES 15	0.45	Moderate
VES 16	0.32	Moderate
VES 17	0.44	Moderate
VES 18	0.13	Weak
VES 19	0.04	Poor
VES 20	0.09	Poor

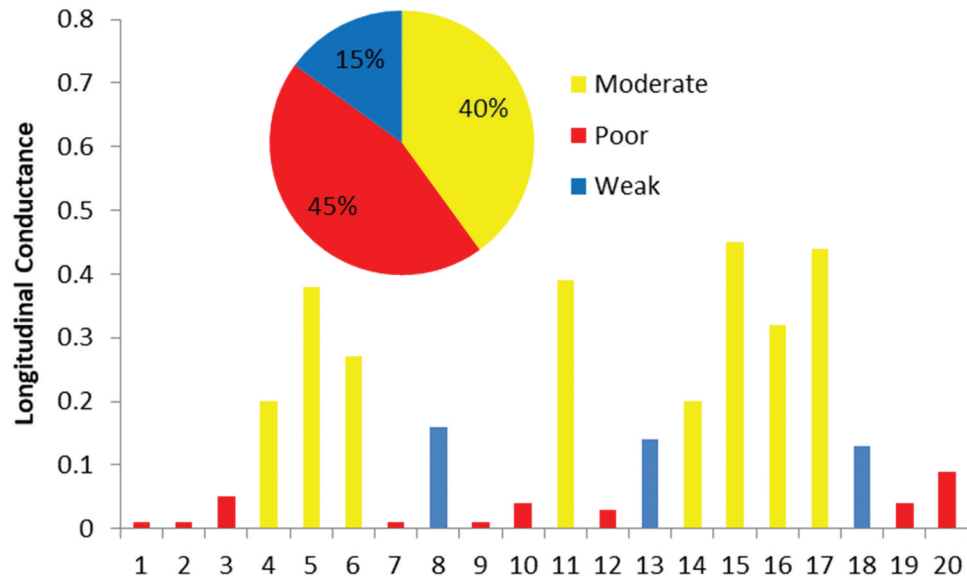


**Figure 11.** Infographic representation of the longitudinal conductance and protective capacity ratings of the established VES points at the study dumpsite.

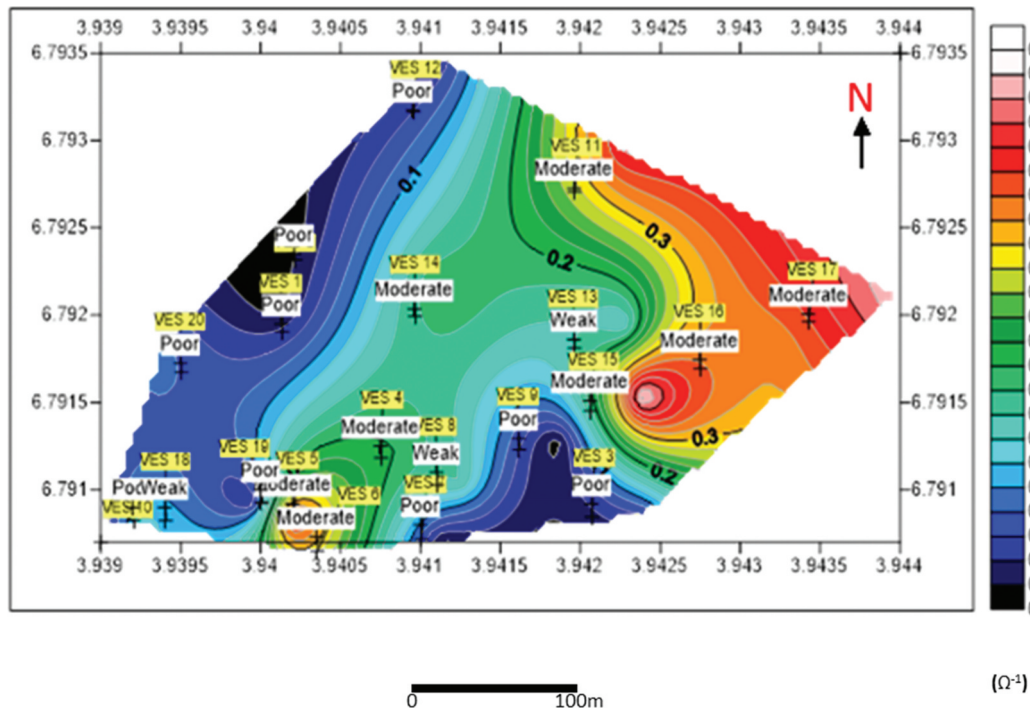


**Figure 12.** Total longitudinal conductance map of the study area.

## 5. Conclusion

The interpretation of the data obtained conclusively revealed that the southwestern part of the study area shows a high degree of contamination at current electrode depths of 0.6 and 5.4 m. The northern part shows a considerable level of contamination, while the depth of 5.4 m shows a relatively high resistivity value, indicating low or no degree of leachate infiltration. The calculated longitudinal conductance of the study area ranges between 0.01 and 0.45  $\Omega^{-1}$ , which is an indication of a poor to

moderate protective capacity rating, which shows that leachate can easily move/infiltrate through the subsurface of the study area. The protective capacity rating can also be link to the geology of the study area because of the presence of sandstone, which has high porosity, which is a typical characteristic of a sedimentary basin, as in the study area. Determinately, the overlying lithological unit within the study area has been filled with leachate to shallow depths far from the water level, thereby depicting the safety of the groundwater in the study area.


## Disclosure statement


No potential conflict of interest was reported by the author(s).

## ORCID

Ganiyu Omotola Mosuro  <http://orcid.org/0000-0002-7336-4863>

Olateju Olatunji Bayewu  <http://orcid.org/0000-0003-3922-0185>

Oluwadamilare Oluwatobiloba Odugbesan  <http://orcid.org/0000-0001-8448-4708>

Moroof Olusunbo Oloruntola  <http://orcid.org/0000-0001-7760-9365>

## References

- Abdullahi NK, Osazuwa IB, Sule PO, Onugba A. 2013. Geophysical assessment of an active open dump site in basement complex of Northwestern Nigeria. *Int J Eng Sci Inv.* 2(5):2319–6726.
- Aboh HO. 2001. Detailed regional geophysical investigation of the subsurface terrain in Kaduna Area, Kaduna state [Unpublished PhD thesis]. Zaria: Department of Physics, Ahmadu Bello University.
- Adebisi NO, Bayewu OO, Ariyo SM, Go OM, Alaka AO, Odugbesan OO, Odugbesan OO. 2022. Assessment of environmental pollution using electrical resistivity and logging techniques over a municipal dumpsite of Ijagun Ijebu Ode. *Iraqi J Sci Technol.* 63(3):1071–1090. doi: 10.24996/ijst.2022.63.3.16.
- Akanni CO, Odugbemi SO, Oyesiku OO, Ademiluyi OO. 2000. Physical environment in Onakomaiya. In: I A, editor. *Ogun state local and regional perspectives, centre for sandwich programmes (CESAP)*. Avebury: Ogun state university, Ago-Iwoye, Ashgate publishing Ltd; p. 14–25.
- Ayolabi EA, Badmus BS. 2004. Hydrogeological Significance of Geoelectric Sounding at Ijebu-Ode Area, South West Nigeria. *Global J Geological Sci.* 2(1):67–77. <http://ajol.info/index.php/gjgs/article/view/18683>.
- Bakare W. 2020. Solid waste management in Nigeria. [accessed 2020 Mar 31] from <https://www.bioenergyconsult.com/solid-waste-nigeria/>.
- Bayode S, Omosuyi GO, Mogaji KA, Adebayo ST. 2011. Geoelectric mapping of some ancient dumpsites and the associated pollution plume in Akure Metropolis, Southwestern Nigeria. *Int J Phys Sci.* 3(1):68–80.
- Billman HG. 1976. Offshore stratigraphy and paleontology of the Dahomey embayment. *Proceedings of the 7th African Micropaleontological Colloquium*; Nigeria: Ile-Ife.
- Blaricom RDV. 2002. Ultra-High Resolution Shallow Resistivity Survey Using Corrected Resistivity (C Rho.) Field Procedures and Equation. In: *Symposium on the Application of Geophysics to Engineering and Environmental Problems 2002*. Society of Exploration Geophysicists; p. HRR1–HRR1.
- Gholam LR, Mohammad N. 2005. Geoelectrical investigation for the assessment of groundwater conditions: a case study. *Ann Of Geophysics.* 48(6):937–944.
- Henriet JP. 1976. Direct application of Dar Zarrouk parameters in groundwater survey. *Geophys Prospect.* 24(2):344–353. doi: 10.1111/j.1365-2478.1976.tb00931.x.
- Ibitola MP, Ehinola OA, Akininbagbe AE. 2011. Electrical resistivity method in delineating vadose and saturated zone in some selected dumpsites in Ibadan part of South-Western, Nigeria. *Int J Geomatics And Geosciences.* 2(1):164.
- Meju MA. 2000. Geoelectrical investigation of old/abandoned, covered landfill sites in urban areas: model development with a genetic diagnosis approach. *J Appl Geophysics.* 44(2–3):115–150. doi: 10.1016/S0926-9851(00)00011-2.
- Mosuro GO, Bayewu OO, Odugbesan OO, Hassan Y, Adebola AI, Oloruntola OM. 2019. Mapping subsurface leachate migration path using 3D electrical resistivity imaging at Farri dumpsite, Ijebu Ode, Southwestern Nigeria. *J Earth Atmos Res.* 2(1):95–102.
- Obaje NG. 2009. In: S. Bhattacharji, H. J. Neugebauer, J. Reitner, K. Stuwe, editors. *The Dahomey Basin*, 103–108. Berlin, Heidelberg: Springer.
- Okeke OC, Abiahu CMG, Anifowose FA, Fagorite VI. 2019. A review of the geology and mineral resources of Dahomey Basin, Southwestern Nigeria. *Int J Environ Sci And Nat Resour.* 21(1):1–5. doi: 10.19080/IJESNR.2019.21.556055.
- Okusun EA. 1990. A review of the Cretaceous stratigraphy of the Dahomey Embayment, West Africa. *Cretaceous Res.* 11(1):17–27. doi: 10.1016/S0195-6671(05)80040-0.
- Oluwafemi O. 2012. The role of geophysics in the investigation of waste disposal site in Ikare-Akoko area, Southwestern Nigeria. *Int J Sci Emerg Technol [Internet].* 4(5):181–204.
- Omatsola ME, Adegoke OS. 1981. Tectonic evolution and Cretaceous stratigraphy of the Dahomey basin. *J Min Geol.* 8:130–137.
- Onakomaiya SO, Oyesiku K, Jegede FJ. 1992. *Ogun State in maps 187*. Ibadan: Rex Charles Publications.
- Reynolds JM. 2003. *An introduction to applied and environmental geophysics*. (UK): John Wiley and Sons. Reynolds Geosciences Limited.
- Samouëlian A, Cousin I, Tabbagh A, Bruand A, Richard G. 2005. Electrical resistivity survey in soil science: a review. *Soil And Tillage Res.* 83(2):173–193. doi: 10.1016/j.still.2004.10.004.
- Smith VR. 1992. *The Paparua Landfill: Hydrogeological, geophysical and hydrogeochemical investigations of groundwater contamination by leachate*, Christchurch New Zealand [PhD thesis]. University of Canterbury.
- Yusuf MA, Abiye TA. 2019. Risks of groundwater pollution in the coastal areas of Lagos, southwestern Nigeria. *Groundwater For Sustain Devel.* 9:100222. doi: 10.1016/j.gsd.2019.100222.